Journal of Modern Optics
Vol. 54, Nos. 16–17, 10–20 November 2007, 2339–2349

Fidelity of optimally controlled quantum gates with randomly coupled multiparticle environments

MATTHEW D. GRACE*†, CONSTANTIN BRIF†,
HERSCHEL RABITZ†, DANIEL A. LIDAR‡,
IAN A. WALMSLEY§ and ROBERT L. KOSUT¶

†Department of Chemistry, Princeton University, Princeton,
New Jersey 08544, USA
‡Departments of Chemistry, Electrical Engineering, and Physics,
University of Southern California, Los Angeles, CA 90089, USA,
§Department of Physics, University of Oxford, Oxford OX1 3PU, UK
¶SC Solutions, Inc., 1261 Oakmead Parkway, Sunnyvale, CA 94085, USA

(*Received 7 March 2007; in final form 14 August 2007*)

This work studies the feasibility of optimal control of high-fidelity quantum gates in a model of interacting two-level particles. One particle (the qubit) serves as the quantum information processor, whose evolution is controlled by a time-dependent external field. The other particles are not directly controlled and serve as an effective environment, coupling to which is the source of decoherence. The control objective is to generate target one-qubit gates in the presence of strong environmentally-induced decoherence and under physically motivated restrictions on the control field. It is found that interactions among the environmental particles have a negligible effect on the gate fidelity and require no additional adjustment of the control field. Another interesting result is that optimally controlled quantum gates are remarkably robust to random variations in qubit-environment and inter-environment coupling strengths. These findings demonstrate the utility of optimal control for management of quantum-information systems in a very precise and specific manner, especially when the dynamics complexity is exacerbated by inherently uncertain environmental coupling.

1. Introduction

The methods of optimal control are very useful for effectively managing various quantum systems [1, 2] and are particularly important in situations requiring precise quantum operations, as is the case for quantum computation (QC) [3]. One of the most difficult problems of QC is that unavoidable coupling of the quantum information processor (QIP) to the environment results in a loss of coherence.

*Corresponding author. Email: mgrace@princeton.edu

Journal of Modern Optics
ISSN 0950–0340 print/ISSN 1362–3044 online © 2007 Taylor & Francis
http://www.tandf.co.uk/journals
DOI: 10.1080/09500340701639615

In recent years, significant attention was devoted to various methods of dynamic suppression of environmentally-induced decoherence in open quantum systems, including applications of pre-designed external fields [4–8] and optimal control techniques [9–15]. In a separate line of research, several works [16–21] considered the generation of optimally controlled unitary quantum gates in ideal situations where coupling to the environment can be neglected during the gate operation.

The optimal control of quantum gates in the presence of decoherence still remains to be fully explored. Two recent works [22, 23] discussed specific techniques, involving optimizations over sets of controls operating in pre-designed 'weak-decoherence' subspaces. We recently proposed [24] a different approach in which the full power of optimal control theory is used to generate the target gate transformation with the highest possible fidelity while simultaneously suppressing decoherence induced by coupling to a multiparticle environment. This method does not rely on any special pre-design of system parameters to weaken decoherence (e.g. using tunable inter-qubit couplings as in [22] or auxiliary qubits as in [23]); the only control used in our approach is a time-dependent external field. A similar application of optimal control was also recently considered in [25] for another model of a decohering environment. Optimization techniques were also applied recently to quantum error correction (QEC) [26,27]. In contrast to QEC, our approach does not require ancilla qubits and is not limited to the weak decoherence regime. The optimal control of quantum gates can potentially be used in conjunction with QEC to achieve fault tolerance with an improved threshold.

In the previous work [24], we showed that optimal control fields, found by employing a combination of genetic and gradient algorithms, are able to produce high-fidelity quantum gates in the presence of strong decoherence. Optimal solutions revealed interesting control mechanisms that utilize dynamic Stark shifts to weaken coupling to the environment and control-induced revivals to restore coherence. In the present work, we extend the analysis of optimally controlled quantum gates to situations where (i) the environmental particles interact with each other and (ii) couplings between the QIP and environment and within the environment itself have randomly varied strengths. Taking into account these additional environmental effects makes our model more closely related to realistic quantum information systems (in particular, spin-based solid-state realizations of QC [28–32]). An interesting finding is that the effect of inter-environment interactions on the fidelity of optimally controlled quantum gates is negligible (potentially allowing one to neglect certain interaction terms in the Hamiltonian). We also demonstrate that the optimal control generates quantum gates which are inherently robust to random variations in qubit-environment and inter-environment coupling strengths.

2. Model system

We use a model of interacting two-level particles (e.g. spin-half particles or two-level atoms), which are divided into the QIP, composed of one qubit, and an n-particle environment. The qubit is directly coupled to a time-dependent external control field, while the environment is not directly controlled and is managed only through its

interaction with the qubit. The evolution of the composite system of the qubit and environment is treated in an exact quantum-mechanical manner, without either approximating the dynamics by a master equation or using a perturbative analysis based on the weak coupling assumption. The Hamiltonian for the controlled system, $H = H_0 + H_C + H_{\text{int}}$, has the form ($\hbar = 1$)

$$H = \sum_{i=0}^{n} \omega_i S_{iz} - \mu C(t) S_{0x} - \sum_{i<j} \gamma_{ij} \mathbf{S}_i \cdot \mathbf{S}_j. \tag{1}$$

Here, $i = 0$ labels the qubit and $i = 1, \ldots, n$ label the environmental particles, $\mathbf{S}_i = (S_{ix}, S_{iy}, S_{iz})$ is the spin operator for the ith particle ($\mathbf{S}_i = (1/2)\boldsymbol{\sigma}_i$, in terms of the Pauli matrices), H_0 is the sum over the free Hamiltonians $\omega_i S_{iz}$ for all $n+1$ particles (ω_i is the transition angular frequency for the ith particle), H_C specifies the coupling between the qubit and the time-dependent control field $C(t)$ (μ is the dipole moment), and H_{int} represents the Heisenberg exchange interaction between the particles (γ_{ij} is the coupling parameter for the ith and jth particles). This model is particularly relevant to spin-based solid-state realizations of quantum gates (see, e.g. [28–32]), in which unwanted interactions exist due to impurities in semiconductor structures or usage of relatively dense lattices of spin-like qubits (e.g. electron spins in an array of quantum dots or electrons on liquid helium).

In this work, we optimize one-qubit gates coupled to n-particle environments ($n = 1, 2, 4, 6$). For $n = 2$, the system can be modelled as a two-dimensional triangular lattice with the qubit q_0 coupled to two environmental particles e_1 and e_2:

$$\begin{array}{ccccc} & & q_0 & & \\ \gamma_{01} & \swarrow\!\nearrow & & \nwarrow\!\searrow & \gamma_{02}\,. \\ & & \gamma_{12} & & \\ e_1 & & \longleftrightarrow & & e_2 \end{array} \tag{2}$$

For $n = 4$, the system can be modelled as a two-dimensional lattice with the qubit q_0 at the centre, coupled to four environmental particles $\{e_1, \ldots, e_4\}$:

$$\begin{array}{ccccccc} & & & e_3 & & & \\ & & \swarrow\!\nearrow & \updownarrow & \nwarrow\!\searrow & & \\ e_1 & \longleftrightarrow & & q_0 & & \longleftrightarrow & e_2\,. \\ & & \nwarrow\!\searrow & \updownarrow & \swarrow\!\nearrow & & \\ & & & e_4 & & & \end{array} \tag{3}$$

Similarly, for $n = 6$, the system can be modelled as a three-dimensional lattice with the qubit at the centre, coupled to six environmental particles. Since the evolution of the composite system is numerically exact and our optimization procedure (described in section 5 and [24]) is iterative, we limit the number of environmental particles to $n \leq 6$ for computationally tractable simulations.

We will first consider the case of well-specified coupling parameters given by

$$\gamma_{ij} = \begin{cases} \gamma, & \text{for } i = 0 \quad \text{and } j = 1, \ldots, n, \\ \gamma', & \text{for } i = 1, \ldots, n-1, \quad \text{and } j > i, \end{cases} \tag{4}$$

which implies that the qubit interacts with each environmental particle with the coupling parameter γ and environmental particles interact with each other with the

coupling parameter γ' (compare to [24] where $\gamma' = 0$). Then we will consider a more general situation in which every coupling parameter γ_{ij} takes a random value from a normal distribution.

3. Distance measure for evolution operators

Let $U(t) \in \mathrm{U}(2^{n+1})$ be the unitary time-evolution operator of the composite system and $G \in \mathrm{U}(2)$ be the unitary target transformation for the quantum gate. The evolution is governed by the Schrödinger equation, $\dot{U}(t) = -\mathrm{i}H(t)U(t)$, with the initial condition $U(0) = I$. The gate fidelity depends on the distance between the actual evolution $U \equiv U(t_\mathrm{f})$ at the final time t_f and the target transformation G. In order to achieve a perfect gate, it suffices for the time-evolution operator at $t = t_\mathrm{f}$ to be in a tensor-product form $U_\mathrm{opt} = G \otimes \Phi$, where $\Phi \in \mathrm{U}(2^n)$ is an arbitrary unitary transformation acting on the environment. Therefore, the following objective functional is proposed as the measure of the distance between U and G [33]: $J = \lambda_n \min_\Phi \|U - G \otimes \Phi\|$ subject to $\Phi \in \mathrm{U}(2^n)$ (where $\|\cdot\|$ is a matrix norm on the space $M_{2^{n+1}}(\mathbb{C})$ of $2^{n+1} \times 2^{n+1}$ complex matrices and λ_n is a normalization factor). Using the Frobenius norm, defined as $\|A\|_\mathrm{Fr} = [\mathrm{trace}(A^\dagger A)]^{1/2}$, and $\lambda_n = 2^{-(n+2)/2}$, the distance measure becomes [33]

$$J = \left[1 - 2^{\lambda_n^2}\ \mathrm{trace}\left((Q^\dagger Q)^{1/2}\right)\right]^{1/2}, \tag{5}$$

$$Q_{\nu\nu'} = \sum_{r,r'=1}^{2} G^*_{rr'} U_{rr'\nu\nu'}, \tag{6}$$

where $Q \in M_{2^n}(C)$ and $Q_{\nu\nu'}$, $G_{rr'}$, and $U_{rr'\nu\nu'}$ are elements of the matrix representations of Q, G and U, respectively. Since $0 \leq J \leq 1$, it is convenient to define the gate fidelity as $F = 1 - J$. An important property of this distance measure is its independence of the initial state. In contrast to some other distance measures [3], J is evaluated directly from the evolution operator U, with no need to specify the initial state of the system. This property of J reflects our objective of generating a specified target transformation for whatever initial state, pure or mixed, direct-product or entangled.

4. Measure of decoherence and system parameters

A useful measure of decoherence is the von Neumann entropy: $S_\mathrm{vN}(t) = -\mathrm{trace}\{\rho_\mathrm{q}(t)\ln[\rho_\mathrm{q}(t)]\}$, where $\rho_\mathrm{q}(t)$ is the reduced density matrix for the qubit, $\rho_\mathrm{q}(t) = \mathrm{trace}_\mathrm{env}(\rho(t))$. For a pure state, $S_\mathrm{vN} = 0$, while for a maximally mixed state of a k-level system, $S_\mathrm{vN} = \ln(k)$. The initial state used for the entropy calculations is $|\Psi(0)\rangle = |-\rangle_0 \otimes \bigotimes_{i=1}^{n} |+\rangle_i$, where $S_{iz}|\pm\rangle_i = \pm(1/2)|\pm\rangle_i$. The distance measure J of equation (5) is independent of the initial state and consequently so are the optimal control fields found for the target gates and the corresponding fidelities.

Therefore, the specific choice of the initial state for the entropy calculations places no limitations whatsoever on the generality of the optimal control results.

For the optimal control simulations below, the system parameters are chosen to ensure complex dynamics and strong decoherence: values of γ/ω are up to 0.02, which is significant for QC applications, and frequencies ω_i are close (but not equal) to enhance the interaction. We define the unit of time and introduce a natural system of units by choosing the qubit frequency $\omega_0 = 1$ for all simulations (implying that one period of free evolution is 2π). The frequencies of the environmental particles are: $\omega_1 \approx 0.99841$, $\omega_2 \approx 1.00159$, $\omega_3 \approx 0.96007$, $\omega_4 \approx 1.04159$, $\omega_5 \approx 0.87597$, $\omega_6 \approx 1.14159$ (see [24] for details). Imposing upper limits on the gate duration ($t_f \leq 60$) and coupling parameter ($\gamma \leq 0.02$) places the dynamics of the uncontrolled system in the regime where decoherence increases monotonically with time (before the entropy reaches its maximum value of $S_{vN} \approx \ln 2$). This dynamical regime approximates some of the effects that the QIP would experience from a larger environment, in particular, preventing restoration of coherence to the qubit by uncontrolled revivals. Thus, any increase in coherence may be attributed exclusively to the action of the control field.

5. Optimization procedure

Combined genetic and gradient algorithms are employed to minimize the distance measure J of equation (5) (or, equivalently, to maximize the fidelity F) with respect to the control field $C(t)$. The target quantum logical transformation is the one-qubit Hadamard gate (an element of a universal set of logical operations for QC [3]).

When a genetic algorithm is used, the gate fidelity F is maximized with respect to a parameterized control field $C(t) = f(t)\sum_\ell A_\ell \cos(\tilde{\omega}_\ell t + \theta_\ell)$. Here, $f(t)$ is an envelope function incorporating the field's spectral width and A_ℓ, $\tilde{\omega}_\ell$ and θ_ℓ are the amplitude, central frequency, and relative phase of the ℓth component of the field, respectively. A combination of these parameters ('genes') represents an 'individual' (whose 'fitness' is the gate fidelity), and a collection of individuals constitutes a 'population' (we use population sizes of ~250).

Removing the constraints on the control field imposed by the parameterized form above provides the potential for more effective control of the system. In this case the optimal control field is found by minimizing the following functional [17,18]:

$$K = J + \mathrm{Re}\int_0^{t_f} \mathrm{trace}\left\{[\dot{U}(t) + iH(t)U(t)]B(t)\right\}dt + \frac{\alpha}{2}\int_0^{t_f} \left|C(t)\right|^2 dt. \tag{7}$$

Upon minimization of K, the first integral term constrains $U(t)$ to obey the Schrödinger equation ($B(t)$ is an operator Lagrange multiplier) and the second integral term penalizes the field fluence $\mathcal{E} = \int_0^{t_f} |C(t)|^2\, dt$ with a weight $\alpha > 0$. Applying the calculus of variations to K with respect to $B(t)$ and $U(t)$ yields the Schrödinger equation for $U(t)$ and the time-reversed Schrödinger equation for $B(t)$: $\dot{B}(t) = iB(t)H(t)$, with an appropriate final time condition. The optimal field is found iteratively, using a gradient algorithm (see [24] for optimization details).

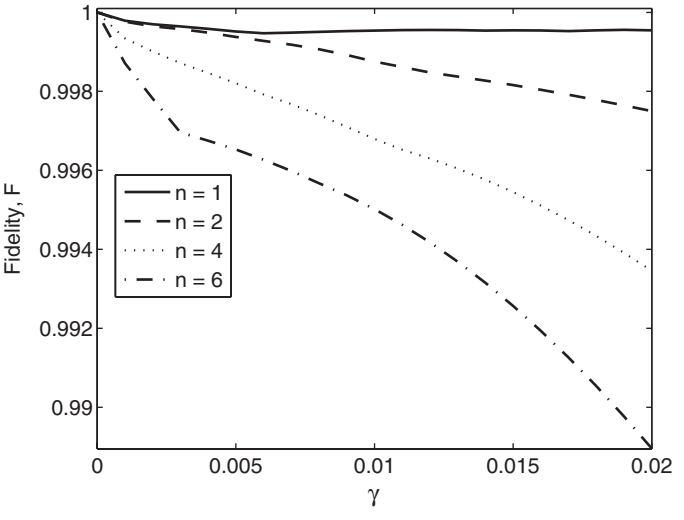

Figure 1. The gate fidelity F versus the qubit-environment coupling parameter γ, for the Hadamard gates optimally controlled in the presence of n-particle environments ($n = 1, 2, 4, 6$). Values of γ range from 0 to 0.02 in increments of 0.001.

Despite the lack of direct coupling of the control field to the environment, it can be shown that the composite system described by equation (1) is completely controllable (up to a global phase), as defined in [34]. However, the restrictions on the gate duration and on the shape of the control field limit the achievable fidelity.

6. Results: optimally controlled one-qubit gate with multiparticle environments

Fidelities of one-qubit Hadamard gates optimized in the presence of n-particle environments ($n = 1, 2, 4, 6$) are presented in figure 1 for $\gamma' = 0$ and various values of the qubit-environment coupling parameter γ. For a one-particle environment, the control fields optimized for the actual values of γ result in fidelities at least above 0.9994. In particular, we obtain $F > 1 - 10^{-6}$ for $\gamma = 0$ (a closed system) and $F \approx 0.9995$ for $\gamma = 0.02$ (the strongest coupling considered). However, it becomes more difficult to counteract decoherence as the number of the environmental particles increases; as seen in figure 1, for larger values of n the gate fidelity decreases more rapidly (faster than linearly) as γ increases. We also find that applying a control field optimized for a one-particle environment ($n = 1$) to $n \geq 2$ results in a significant fidelity loss (up to 10% of the original value). This demonstrates the dependence of the optimal control on the size of the environment.

Optimal control field parameters, gate fidelity, and final-time entropy for the Hadamard gate coupled to n-particle environments ($n = 1, 2, 4, 6$, $\gamma = 0.02$, and $\gamma' = 0$) are reported in table 1. The fields are intense, with maximum amplitudes ranging from approximately 2.0 (for $n = 1$) to 3.9 (for $n = 2$). The exact time structure of the optimal field is not intuitive and is delicately adjusted to the particular

Table 1. Optimal control field parameters (the maximum field amplitude $A_{\max}$, control duration t_f, and field fluence $\mathcal{E}$), gate fidelity F, and final-time entropy $S_{vN}(t_f)$ for the Hadamard one-qubit gates coupled to n-particle environments ($n = 1, 2, 4, 6$ and $\gamma = 0.02$). The initial state for the entropy computation is $|\Psi(0)\rangle$.

	n			
	1	2	4	6
$A_{\max}$	2.0	3.9	3.8	3.1
t_f	25.0	15.4	25.0	30.0
$\mathcal{E}$	20.0	49.0	55.5	54.5
F	0.9995	0.9975	0.9935	0.9890
$S_{vN}(t_f)$	8.6×10^{-8}	4.4×10^{-5}	4.7×10^{-4}	2.4×10^{-3}

control application. For example, control fields optimized for $\gamma = 0.02$ are not only more intense than those optimized for $\gamma = 0$, they also have very different structures. We also find that high-fidelity optimal solutions for $\gamma = 0$ are obtained for control pulse durations $t_f \approx 12.0$. In comparison, for $\gamma = 0.02$, high-fidelity optimal solutions are obtained at longer pulse durations (cf. results reported in table 1, e.g. $t_f = 15.4$ for $n = 2$ and $t_f = 25.0$ for $n = 1$ and $n = 4$). When the qubit-environment interaction is on, the control field is required to generate the target gate transformation and at the same time counteract decoherence. As described below, the control accomplishes the latter goal by restoring coherence to the QIP and therefore longer pulse durations are needed in the presence of environmental coupling. As mentioned above, there are also significant differences in the control fields optimized for different numbers of environmental particles.

We also would like to explore how interactions among the environmental particles affect optimally controlled gate operations. Interestingly, we find that for a given n-particle environment ($n \geq 2$ and $\gamma = 0.02$), some optimal control solutions obtained for $\gamma' \neq 0$ (e.g. $\gamma' = (7/8)\gamma = 0.0175$) are essentially identical to the solutions found for $\gamma' = 0$. This means that no additional adjustment of the control field is necessary to account for the effect of inter-environment couplings. Moreover, applying these optimal control fields to the systems with $\gamma' \neq 0$ yields approximately the same gate fidelity, as seen for $\gamma' = 0$ (the actual decreases in the fidelity observed for $\gamma' = (1/2)\gamma$ and $\gamma' = (7/8)\gamma$ are of the order of 10^{-5} for $n = 2$ and 10^{-4} for $n = 4$).

Control mechanisms can be better understood by examining the decoherence dynamics of the qubit. Figure 2 shows the time behaviour of the von Neumann entropy of the qubit for the optimally controlled evolution, with $\gamma = 0.02$, $\gamma' = 0.0175$, and $n = 2, 4$. The difference between the entropy values for $\gamma' \neq 0$ and $\gamma' = 0$ is extremely small, implying that the same control mechanism works in both cases. We observe that the optimal control dramatically enhances coherence of the qubit system in comparison to the uncontrolled dynamics. Decoherence is suppressed by the control at all times, but especially at the end of the transformation. For example, for the Hadamard gate with $\gamma = 0.02$, $S_{vN}(t_f) < 10^{-7}$ in the presence of a one-particle environment, which means that at $t = t_f$ the qubit and environment are almost uncoupled. While the value of $S_{vN}(t_f)$ increases with the environment size

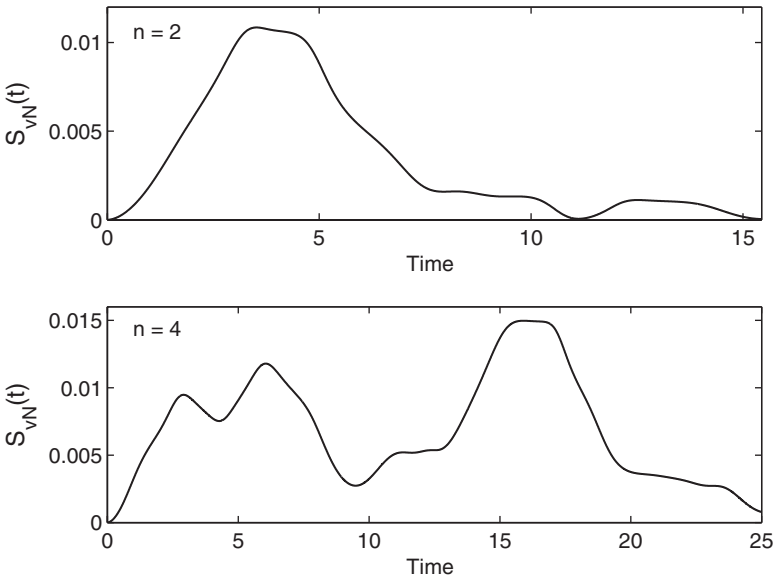

Figure 2. The von Neumann entropy $S_{vN}(t)$ versus time, for the optimally controlled Hadamard gates coupled to two- and four-particle environments ($n = 2, 4$, $\gamma = 0.02$, and $\gamma' = 0.0175$). The initial state for the entropy computation is $|\Psi(0)\rangle$.

(see table 1), the optimal control is still able to achieve a significant degree of decoupling at the final time. Inspecting eigenvalues of the controlled Hamiltonian, we find that the intense control field creates significant dynamic Stark shifts of the energy levels. This effect is mainly responsible for reducing the qubit-environment interaction during the control pulse. However, achieving extremely low final-time entropies and correspondingly high gate fidelities requires the employment of an induced coherence revival. In the uncontrolled system, revivals occur at times much longer than t_f, so that the strong coherence revival observed at $t = t_f$ is induced exclusively by the control field. However, as the complexity of the composite system increases, it becomes more difficult to induce an almost perfect revival; therefore, the gate fidelity and final-time coherence decrease as n increases. Similar results are found for a two-qubit controlled-NOT gate optimized in the presence of a one-particle environment, in which case we observe [24] a longer pulse duration ($t_f = 121.1$) and smaller fidelity ($F \approx 0.9798$) than for one-qubit gates.

7. Robustness of optimally controlled gates to coupling-strength variations

In realistic quantum systems, the strength of coupling between particles cannot always be accurately measured and is also subject to fluctuations caused by noise or variations due to imperfect manufacturing or preparation. Therefore, it is important to explore the effect of general symmetry-breaking variations in the coupling parameters γ_{ij} on operations of optimally controlled quantum gates. Given the

Table 2. Fidelity and entropy data for the one-qubit Hadamard gate, obtained when the control field optimized for a specified set of the system parameters is applied to an ensemble of systems with normally distributed variations in the coupling parameters γ_{ij}. Columns of F and $S_{\mathrm{vN}}(t_{\mathrm{f}})$ contain fidelity and final-time entropy values, respectively, obtained for the specified coupling strengths: $\gamma = 0.02$ and $\gamma' = c\gamma$ ($c = 0, 1/2, 7/8$). Columns of $\overline{F}$ and $\overline{S_{\mathrm{vN}}}$ contain mean values of the fidelity and final-time entropy, respectively, over the ensemble, while σ_F and $\sigma_{S_{\mathrm{vN}}}$ are the respective standard deviations.

γ'	F	$\overline{F}$	σ_F	$S_{\mathrm{vN}}(t_{\mathrm{f}})$	$\overline{S_{\mathrm{vN}}}$	$\sigma_{S_{\mathrm{vN}}}$
$n = 2$						
$\gamma' = 0$	0.9975	0.9975	2.6×10^{-4}	4.4×10^{-5}	4.6×10^{-5}	1.5×10^{-5}
$\gamma' = (1/2)\overline{\gamma}$	0.9975	0.9975	2.6×10^{-4}	4.5×10^{-5}	4.6×10^{-5}	1.5×10^{-5}
$\overline{\gamma'} = (7/8)\overline{\gamma}$	0.9975	0.9975	2.6×10^{-4}	4.5×10^{-5}	4.7×10^{-5}	1.5×10^{-5}
$n = 4$						
$\gamma' = 0$	0.9935	0.9934	6.1×10^{-4}	4.7×10^{-4}	4.8×10^{-4}	8.1×10^{-5}
$\overline{\gamma'} = (1/2)\overline{\gamma}$	0.9934	0.9933	6.3×10^{-4}	6.4×10^{-4}	6.5×10^{-4}	1.4×10^{-4}
$\overline{\gamma'} = (7/8)\overline{\gamma}$	0.9933	0.9931	6.5×10^{-4}	7.8×10^{-4}	8.1×10^{-4}	2.1×10^{-4}

one-qubit Hadamard gate as the target transformation and a fixed number n of environmental particles ($n = 2, 4$), we find the optimal control field for a specified set of coupling parameters γ_{ij} of equation (4), with $\gamma = 0.02$ and $\gamma' = c\gamma$ ($c = 0, 1/2, 7/8$). Then we apply this control field to an ensemble of systems with normally distributed variations in the coupling parameters γ_{ij} and analyse how the uncertainty in the coupling strengths affects the gate fidelity and final-time entropy. Although the dependence of F and $S_{\mathrm{vN}}(t_{\mathrm{f}})$ on the coupling parameters is nonlinear (which implies that the corresponding distributions of F and $S_{\mathrm{vN}}(t_{\mathrm{f}})$ will not be normal), our statistical analysis employs only mean values and standard deviations, given by $\overline{F} = L^{-1}\sum_{p=1}^{L} F_p$ and $\sigma_F = [L^{-1}\sum_{p=1}^{L}(F_p - \overline{F})^2]^{1/2}$, respectively, for the gate fidelity F, and similarly for the final-time entropy $S_{\mathrm{vN}}(t_{\mathrm{f}})$. The summation is over all elements of the ensemble (ensemble sizes L of the order of 10^5 are used in the calculations).

For each element of the statistical ensemble, the value of each qubit-environment coupling parameter γ_{0j} ($j = 1, \ldots, n$) is randomly selected from the normal distribution with a mean $\overline{\gamma} = 0.02$ and a standard deviation $\sigma_\gamma = \overline{\gamma}/8 = 0.0025$. Analogously, for non-zero inter-environment coupling,† the value of each coupling parameter γ_{ij} ($i = 1, \ldots, n-1$, $j > i$) is also randomly selected from the normal distribution with a mean $\overline{\gamma'} = c\gamma$ and a standard deviation $\sigma_{\gamma'} = \overline{\gamma'}/8 = c\overline{\gamma}/8$. The statistical analysis of the corresponding fidelity and final-time entropy distributions is reported in table 2 (for $n = 2, 4$), and frequency histograms of these distributions are shown in figure 3 (for $n = 4$). These results demonstrate a high degree of robustness of the optimally controlled gates to relatively large variations in the qubit-environment and inter-environment coupling strengths. For given values of n, $\overline{\gamma}$, and $\overline{\gamma'}$, on average there is just a minuscule decrease in the fidelity and final-time coherence due to the coupling strength variations,

†In the case of zero inter-environment coupling, $c = 0$, all zero values of γ_{ij} are left unchanged.

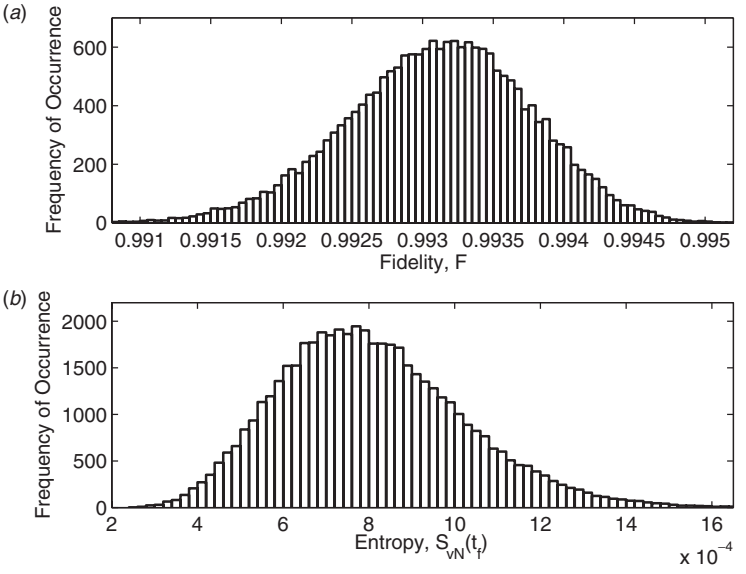

Figure 3. Frequency histograms for (*a*) the gate fidelity distribution and (*b*) the final-time entropy distribution. These distributions are obtained when the control field optimized for the Hadamard gate with $n=4$, $\gamma=0.02$, and $\gamma'=(7/8)\gamma=0.0175$ is applied to an ensemble of systems with normally distributed variations in the coupling parameters γ_{ij}, as explained in the text. Table 2 reports statistical data for these distributions. Note that the sub-plots have different scales for the axes.

and the relative width of the fidelity distribution, $\sigma_F/\overline{F}$, is smaller than $\sigma_\gamma/\overline{\gamma}$ by several orders of magnitude. Based on the data in table 2, we also observe that the standard deviations σ_F and $\sigma_{S_{\mathrm{vN}}}$ increase with the number of environmental particles. Table 2 also helps us to see that inter-environment couplings have very little effect on the gate performance, although their influence slightly increases with $\overline{\gamma'}$.

8. Conclusions

This work demonstrates the importance of the optimal control theory for designing quantum gates, especially in the presence of environmentally-induced decoherence. The model studied here represents a realistic system of interacting qubits with uncertain coupling strengths and is relevant for various physical implementations of QC. Very precise optimal solutions obtained in the presence of unwanted couplings reveal control mechanisms which employ fast and intense time-dependent fields to effectively suppress decoherence via dynamic Stark shifting and restore coherence via an induced revival. In addition, these optimal solutions exhibit a significant degree of inherent robustness to random variations in the coupling strengths. It is also found that optimally controlled gate operations are practically unaffected by interactions between the environmental particles. These results further support the use of laboratory closed-loop optimal controls in QC applications.

Acknowledgements

This work was supported by the ARO-QA, DOE, and NSF. DAL was supported by ARO-QA Grant No. W911NF-05-1-0440 and NSF Grant No. CCF-0523675. IAW acknowledges support by the UK QIP IRC funded by EPSRC, and the EC under the Integrated Project QAP funded by the IST directorate as Contract No. 015848.

References

[1] H. Rabitz, R. de Vivie-Riedle, M. Motzkus, *et al*., Science **288** 824 (2000).
[2] I. Walmsley and H. Rabitz, Phys. Today **56** 43 (2003).
[3] M.A. Nielsen and I.L. Chuang, *Quantum Computation and Quantum Information* (Cambridge University Press, Cambridge, UK, 2000).
[4] L. Viola, E. Knill and S. Lloyd, Phys. Rev. Lett. **82** 2417 (1999).
[5] L. Viola, E. Knill and S. Lloyd, Phys. Rev. Lett. **83** 4888 (1999).
[6] L. Viola, E. Knill and S. Lloyd, Phys. Rev. Lett. **85** 3520 (2000).
[7] A.G. Kofman and G. Kurizki, Phys. Rev. Lett. **93** 130406 (2004).
[8] P. Facchi, S. Tasaki, S. Pascazio, *et al*., Phys. Rev. A **71** 022302 (2005), and references therein.
[9] C. Brif, H. Rabitz, S. Wallentowitz, *et al*., Phys. Rev. A **63** 063404 (2001).
[10] W. Zhu and H. Rabitz, J. Chem. Phys. **118** 6751 (2003).
[11] S.E. Sklarz, D.J. Tannor and N. Khaneja, Phys. Rev. A **69** 053408 (2004).
[12] I.A. Grigorenko and D.V. Khveshchenko, Phys. Rev. Lett. **94** 040506 (2005).
[13] H. Jirari and W. Pötz, Phys. Rev. A **72** 013409 (2005).
[14] H. Jirari and W. Pötz, Phys. Rev. A **74** 022306 (2006).
[15] M. Wenin and W. Pötz, Phys. Rev. A **74** 022319 (2006).
[16] G.D. Sanders, K.W. Kim and W.C. Holton, Phys. Rev. A **59** 1098 (1999).
[17] J.P. Palao and R. Kosloff, Phys. Rev. Lett. **89** 188301 (2002).
[18] J.P. Palao and R. Kosloff, Phys. Rev. A **68** 062308 (2003).
[19] N. Khaneja, T. Reiss, C. Kehlet, *et al*., J. Mag. Res. **172** 296 (2005).
[20] M. Grace, C. Brif, H. Rabitz, *et al*., New J. Phys. **8** 35 (2006).
[21] A. Spörl, T. Schulte-Herbrüggen, S.J. Glaser, *et al*., Phys. Rev. A **75** 012302 (2007).
[22] I.A. Grigorenko and D.V. Khveshchenko, Phys. Rev. Lett. **95** 110501 (2005).
[23] T. Schulte-Herbrüggen, A. Spörl, N. Khaneja, *et al*., preprint quant-ph/0609037 (2006).
[24] M. Grace, C. Brif, H. Rabitz, *et al*., J. Phys. B **40** S103 (2007).
[25] P. Rebentrost, I. Serban, T. Schulte-Herbrüggen, *et al*., preprint quant-ph/0612165 (2006).
[26] M. Reimpell and R.F. Werner, Phys. Rev. Lett. **94** 080501 (2005).
[27] R.L. Kosut and D.A. Lidar, preprint quant-ph/0606078 (2006).
[28] G. Burkard, D. Loss and D.P. DiVincenzo, Phys. Rev. B **59** 2070 (1999).
[29] B.E. Kane, Nature **393** 133 (1998).
[30] R. Vrijen, E. Yablonovitch, K. Wang, *et al*., Phys. Rev. A **62** 012306 (2000).
[31] J.R. Petta, A.C. Johnson, J.M. Taylor, *et al*., Science **309** 2180 (2005).
[32] S.A. Lyon, Phys. Rev. A **74** 052338 (2006).
[33] R.L. Kosut, M. Grace, C. Brif, *et al*., preprint quant-ph/0606064 (2006).
[34] V. Ramakrishna, M.V. Salapaka, M. Dahleh, *et al*., Phys. Rev. A **51** 960 (1995).